Journal of Thermal Analysis and Calorimetry, Vol. 96 (2009) 1, 141–145

EFFECT OF HEATING RATES ON TG-DTA RESULTS OF ALUMINUM NANOPOWDERS PREPARED BY LASER HEATING EVAPORATION

L. Chen[1], *W. L. Song*[1,2,*], *J. Lv*[1], *L. Wang*[2] *and C. S. Xie*[1]

[1]State Key Laboratory of Material Processing and Die and Mould Technology, Huazhong University of Science and Technology, Wuhan 430074, P.R. China
[2]Analytical and Testing Center, Huazhong University of Science and Technology, Wuhan 430074, P. R. China

Aluminum (Al) nanopowders with mean diameter of about 50 nm and passivated by alumina (Al_2O_3) coatings were prepared by an evaporation route: laser heating evaporation. Thermal properties of the nanopowders were investigated by simultaneous thermogravimetric-differential thermal analysis (TG-DTA) in dry oxygen environment, using a series of heating rates (5, 10, 20, 30, 50 and 90°C min^{-1}) from room temperature to 1200°C. With the heating rates rise, the onset and peak temperatures of the oxidation rise, and the conversion degree of Al to Al_2O_3 varies. However, the specific heat release keeps relatively invariant and has an average value of 18.1 kJ g^{-1}. So the specific heat release is the intrinsic characteristic of Al nanopowders, which can represent the ability of energy release.

Keywords: *aluminum, energetic materials, nanopowders, reactivity, TG-DTA*

Introduction

Aluminum (Al) powders are commonly added to propellants, explosives and pyrotechnics compositions to add energy to the burning reaction in propellants and to enhance the blast effect of explosives, as well as their underwater performance. Conventional use of Al powders are typically micron-sized, however, the usual problems of using them are agglomeration, uncompleted degree of oxidation and two-phase losses [1]. Recently, Al nanopowders have attracted widespread interest to solve the problems their micro-counterparts meet due to their unusual energetic properties [2, 3]. These are associated with higher specific surface area, higher reactivity, potential ability to store energy in surface defects, and lower melting points [4–6].

Characterization of Al nanopowders including the particle diameters and morphology, oxide layer thicknesses, thermal behavior is important in predicting performance for its applications. Among them, the thermal behavior which can be applied in the evaluation of the reactivity of Al nanopowders is the main characteristic for the application in explosives and propellants. As for the instruments for thermal analysis, simultaneous thermogravimetric and differential thermal analysis (TG-DTA) is a convenient and useful one [7, 8]. However, TG-DTA results vary under different heating rates for a certain type of Al powders [9–11]. Therefore, more work is needed to understand the relationship between thermal behavior and heating rate applied on TG-DTA.

Al nanopowders can be prepared using a variety of techniques, including electro-exploded wire [12, 13], plasma synthesized process [14], sol–gel [15] and heating evaporation [16]. The heating evaporation methods based on vaporization of metals followed by condensation and particle formation have the ability to produce Al nanopowders below 100 nm or even below 50 nm. These evaporation methods distinguish themselves by the heating apparatuses, such as electric cooker, high-frequency induction and laser. A high-frequency power and high-power CO_2 laser were combined as heating source in the laser heating evaporation method to prepare Al nanopowders with mean particle diameter of 50 nm. Then a series of heating rates were applied in the simultaneous TG-DTA to investigate the thermal behavior of Al nanopowders, and then thermal parameters for the estimation of the reactivity of Al nanopowders were discussed.

Experimental

Materials preparation

Al nanopowders were prepared using an evaporation route: laser heating evaporation. As illustrated in Fig. 1, the bulk pure Al (99.6%) was put in a crucible. The chamber was evacuated below 10 Pa and maintained at 2 kPa argon pressure. Then the high-frequency induction power of 5 kW was initiated, and 5 min later,

* Author for correspondence: wulins@126.com

1388–6150/$20.00

Akadémiai Kiadó, Budapest, Hungary
Springer, Dordrecht, The Netherlands

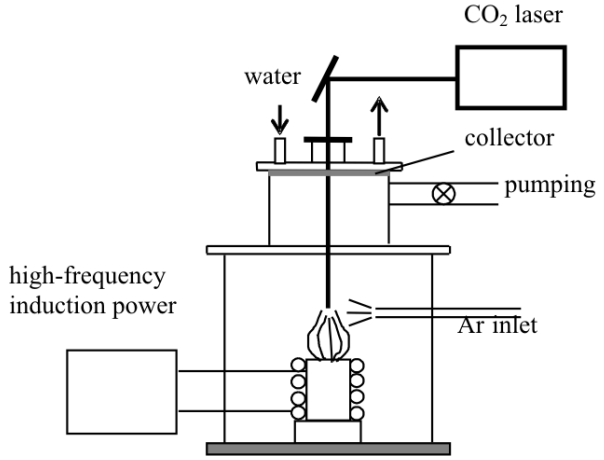

Fig. 1 Schematic diagram of the equipment applied in laser-induction complex heating evaporation

the bulk pure Al was molten. Sequentially, continuous wave CO_2 laser irradiation (with a maximum output of 2 kW) with the power of 1.8 kW was incorporated into the system. After the focused laser beam (4 mm in diameter) radiated on the Al liquid for about one minute, a plasma arc was ignited and rapidly propagated in the reverse direction to the laser beam and in the transverse direction. The plasma expands cools and condenses into clusters, which continue to migrate away from target Al surface until they are collected on the water-cooled wall of the chamber.

The reaction lasted for about 15 min, and then the powers were turned off, simultaneously gas mixture of argon and air (volume ratio about 20:1) was added into the chamber maintaining a pressure of about 320 Pa to passivate Al nanoparticles. Passivating of about 10 h later, the resulting dark gray, air passivated Al nanopowders (about 3.0 g) were collected for further testing and analysis.

Microstructures and thermal analysis

The phases and crystal structures of the powders were analyzed with XRD (PANalytical B.V. X'Pert PRO) using CuKα radiation ($\lambda_{K\alpha 1}$=0.15406 nm), generating voltage 40 kV and current 40 mA. Spectra were collected at a step size of 0.0167° and were scanned from 10 to 90°. The morphology and internal structure of Al nanopowders were investigated using TEM on a Tecnai G2 20 (accelerating voltage 180 kV) and HRTEM on a JEM-2100FEL.

The thermal properties of the as-prepared powders were tested by TG-DTA with a Perkin Elmer TG/DTA 6300 thermal analysis system, which has a maximum heating rate of 100°C min^{-1}. The equipment consists of a pair of horizontal electrobalances, with a 0.1 μg of resolution, a furnace and sensors of temperature, connected to a computer, using the Muse version 5.4U thermal analysis system. The used crucibles were of 70 μL alumina. The samples were heated at different rates of 5, 10, 20, 30, 50 and 90°C min^{-1} from room temperature to 1200°C and all the experiments were carried out under dry oxygen (99.995%) atmosphere, with a fixed gas flow of about 20 mL min^{-1}.

Results and discussion

The general morphologies and structures of Al nanopowders are shown in Figs 2a and b. The low magnification of TEM image Fig. 2a reveals that the produced nanopowders are well dispersed particles with the shape of uniformed sphere and a mean diameter of 50 nm. The high resolution TEM image Fig. 2b shows that the particle has a structure of core-shell: the shell part alumina (Al_2O_3) coats the core Al tightly. The shell part Al_2O_3 with a thickness of about 3 nm was formed in the air passivation process to protect the core Al from intensive oxidation or even spontaneous combustion.

The XRD patterns of air-passivated Al nanopowders are shown in Fig. 3a. The strong diffraction peaks can be indexed to metallic Al and the weak ones correspond to Al_2O_3, which means the sample mainly contains metallic Al and a small quantity of Al_2O_3, which is in good agreement with the HRTEM result of the core-shell structure. No diffraction peaks from other impurities were detected in the sample, which means the high purity of the Al nanopowders.

Thermal properties of the Al nanopowders investigated by simultaneous thermogravimetric-differential thermal analysis (TG-DTA) under a series of heating rates are revealed in Figs 4a and b. The mass of all the samples added into the alumina crucible is of fixed quantification of 1.2±0.1 mg. Seen from the figures, the shape of all the curves can be classified into two types: one is the low heating rates (5, 10, 20°C min^{-1}, Fig. 4a), the other is the high heating rates (30, 50, 90°C min^{-1}, Fig. 4b). There is a mass loss (2–5%) in each TG curves from room temperature to about

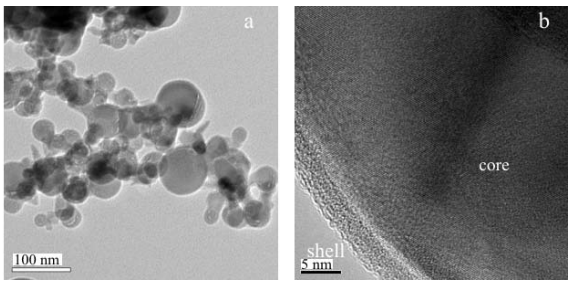

Fig. 2 a – A TEM image of the Al nanopowders; b – An HRTEM image of a single particle

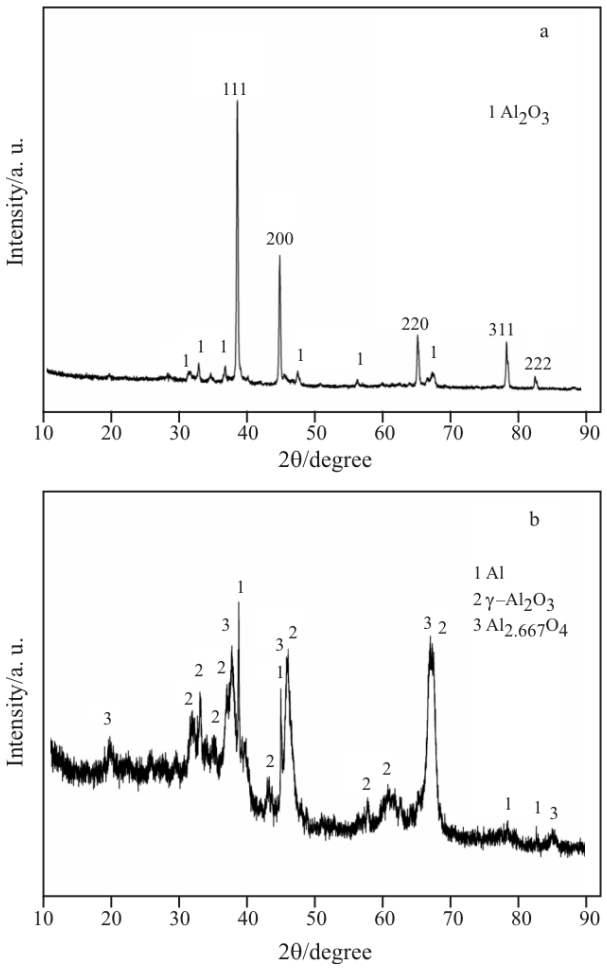

Fig. 3 Results of X-ray diffraction for the powders: a – the as-prepared Al nanopowders; b – collected powders after TG-DTA analysis

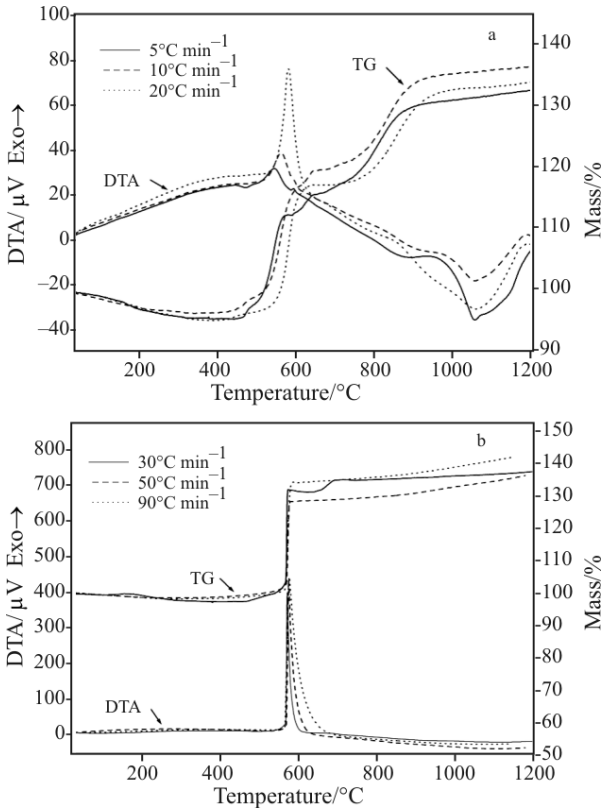

Fig. 4 TG-DTA curves of the Al nanopowders under different heating rates (dry oxygen 20 mL min^{-1}): a – 5, 10, 20°C min^{-1}; b – 30, 50, 90°C min^{-1}

400°C because of the outgassing of the absorbed air (carbon dioxide) and water vapor after preparation of the nanopowders. A general tendency that with the lower heating rates is the more mass loss can also be observed, which means that lower heating rates are propitious to outgas the absorbed substrates in the surface of the nanopowders. Therefore, the mass gain should be calculated from about 400°C after the finish of outgassing. After the mass loss, there is a mass gain in each TG curves especially when the temperature reaches 500–550°C. An intensive mass gain is observed from 500°C (550°C, high heating rates) to 600°C because of the reaction between Al and O_2:

$$4Al(s)+3O_2=2Al_2O_3 \quad (1)$$

For the reaction between Al and O_2, the mass of the samples would increase 1.125 times of the initial mass. The exothermic reaction would occur simultaneously, which can be evidenced by the intensive exothermal peaks in DTA curves.

In the low heating rates, there are two intensive mass gain stages in each TG curve. The first intensive mass gain stage begins at 450°C and finishes at 600°C. The second one ranges from 750 to 900°C. This two-stage mass gain phenomenon can be explained by the mechanism of low temperature oxidation of aluminum nanopowders. The low temperature oxidation of Al particles occurs at least in two steps [17], as illustrated in Fig. 5. The first step, dominated by chemical kinetics, builds a layer (γ-Al_2O_3 and θ-Al_2O_3) of 6 to 10 nm thickness composed of crystallites of the same size independent on the initial particle size. The second step combines diffusion and chemical reaction and proceeds therefore slowly. When the temperature reaches and exceeds 660°C, Al particles melt and expand because the density of the core aluminum decrease from 2.7 kg m^{-3} at solid-state to 2.3 kg m^{-3} at the current liquid state, when Al melts it would expand by 12%. The outer Al_2O_3 shells are in tension,

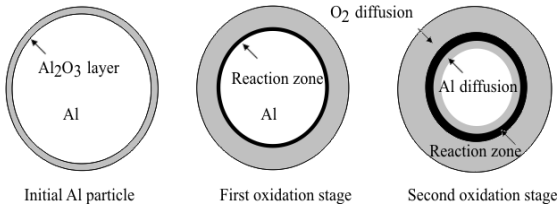

Fig. 5 A schematic representation of the two-stage oxidation mechanism

which is beneficial to the diffusion of the oxygen. The following oxidation step involves the diffusion of oxygen to the metal core and the metal to the outer surface, and the oxygen diffusion is the dominating factor. Then the profile of diffusing oxygen from the surface into the reaction zone front with the metallic fuel is given by (solution of the radial diffusion equation):

$$c_O = c_{O,R} + (c_{O,S} - c_{O,R}) \frac{1 - R/r}{1 - R/R_S} \quad (2)$$

c concentration, r – radius of Al core, R – radius of reaction zone, O – oxygen, S – surface.

The increase of the c_O and tension of Al_2O_3 shell contributes to the second intense mass gain from 750 to 800°C because of the following reaction:

$$4Al(l)+3O_2=2Al_2O_3 \quad (3)$$

In the high heating rates, there is an obvious first mass gain stage in each TG curve, however, the second mass gain is not observed especially in 50 and 90°C min^{-1}. The absence of the second mass gain is due to the more complete oxidation of Al powders in the first oxidation stage or instantaneous combustion because of the rupture of Al_2O_3 shell under the rapid increase of high temperature. The relative high temperature is beneficial for the chemical reaction between Al and oxygen in the first oxidation stage.

Traditionally, the reactivity of Al powders depends on the content of metallic aluminum in powders. However, with the decrease in particle size, the metal content of Al powders usually decreases but the oxidation rate can increase, especially for the nanopowders. Ilyin and Kwon [18, 19] established four parameters obtained from TG-DTA (DSC) to estimate the reactivity of Al powders: the onset temperature of oxidation (T_{on}, °C), the maximum oxidation rate (v_{ox}, mg s^{-1}), the degree of conversion of aluminum in a specified temperature range (α, %), the specific heat release ($S/\Delta m$). The TG-DTA results for the as-prepared Al nanopowders under different heating rates are summarized in Table 1. From Table 1, we can see that with the rise of heating rates, the onset and peak temperature of the first extensive oxidation increase. In the low heating rates, the maximum oxidation rates were calculated from the TG curves. With the rise of heating rates, v_{ox} increases, however, as the mass gain occurred transiently in the high heating rates, the v_{ox} has a high or even infinite value (also can be seen from the tangent of TG curves). It is insignificant to calculate the v_{ox} in high heating rates. The enthalpy change (ΔH) is read by the Muse thermal analysis system from the peak area of each DTA curve. ΔH is a parameter that reveals the heat release of the first oxidation stage. Δm or Δm_1 is the mass percentum increase at the corresponding temperature range in TG curves. The conversion of the Al to Al_2O_3 (α) is 1.125 times of Δm (or Δm_1). From Fig. 3b, we can see that there is unreacted metallic Al in the remained ash after TG-DTA, which means the conversion of the Al is not complete. As the heating rates increase, α_1 increase and α keeps invariant in some degree. From Table 1 and Fig. 4b, we can also see that at the heating rate of 50 °C min^{-1} the values of ΔH, Δm (or α) and Δm_1 (or α_1) are lower even than the values at the heating rate of 30°C min^{-1}. The reason to this phenomenon is that the initial mass (m_i) added into the TG-DTA instrument at 50°C min^{-1} is 1.295 mg which is higher than 1.169 mg at 30°C min^{-1}. More samples make the oxidation of Al nanopowders more incomplete. But this phenomenon can not disturb the tendency summarized above. The last datum listed in the table ($S/\Delta m^*$) is a parameter of specific heat release that can determine the ability of energy release. Specific heat release ($S/\Delta m^*$) means the release of heat per g of Al because of oxidation. Though many parameters of TG-DTA are different with each other under different heating rates, the specific heat release keeps relatively invariant and has an average value of 18.1 kJ g^{-1}. Therefore it is necessary to establish a reasonable heating rate to obtain the parameters to estimate the reactivity of Al nanopowders; however, the specific heat release is a

Table 1 Comparison of TG-DTA results for Al nanopowders under different heating rates

Rates/°C min^{-1}	T_{on}/°C[a]	T_{peak}/°C[b]	v_{ox}/mg s^{-1}	ΔH/kJ g^{-1}	Δm/%[c]	Δm_1/%[d]	$S/\Delta m^*$/kJ g^{-1}[e]
5	493	541	2.27	3.714	37.4	17.5	18.86
10	529	556	2.44	3.548	40.1	16.8	18.77
20	556	578	14.27	4.219	38.9	22.0	17.05
30	566	571	/	6.738	40.4	34.9	17.16
50	560	620	/	6.338	38.0	30.4	18.53
90	564	622	/	7.467	44.0	36.4	18.23

[a]Onset temperature at which a deflection from the established baseline of DTA is observed.
[b]Peak temperature corresponding to a peak value of DTA.
[c]Total mass percentum gain from lowest mass to the end point of the TG curves.
[d]Mass gain percentum for first intensive mass gain obtained between about 400 and 600°C.
[e]$S/\Delta m^*=\Delta H_{mi}/1.125\Delta m_1 m_i=\Delta H/1.125 m_1$, m_i: initial mass of the tested samples.

characteristic parameter for a certain type of Al powders.

Heating rate is an important factor in the thermal calorimetry analysis and there is always a proper heating rate for a specific analyte in a certain calorimetry. Generally, high heating rate benefits the improvement of the sensitivity, while low heating rate helps to improve the resolution of the measurement. As for Al powders which have a special application in energetic materials, such as propellants, explosives or pyrotechnics, have a characteristic of instantaneous combustion in several seconds. So when we investigate or simulate the actual situation of combustion in propellants, the higher heating rates could be applied, however, as we investigate the thermal behavior of Al powders, the lower ones would be proper. From the results above we can also find that a fixed heating rate regardless of high or low should be applied to compare the thermal properties of different types of Al powders.

Conclusions

Crystalline Al nanopowders were synthesized by the laser heating evaporation process. The powders have a uniformed spherical shape, core-shell structure and a mean particle size of 50 nm. After different heating rates applied on TG-DTA, the shape of all the curves can be classified into the low heating rates (5, 10, 20°C min^{-1}) and the high heating rates (30, 50, 90°C min^{-1}). It is obvious that there are two intensive mass gains because of the two-step oxidation of the nanoparticles. The first step (from 450 to 600°C) is dominated by chemical kinetics, the second step, however, combines diffusion and chemical reaction and proceeds slowly. The absence of the second mass gain in the high heating rates is due to the more complete oxidation of Al powders in the first oxidation stage or instantaneous combustion because of the rupture of Al_2O_3 shell under the rapid increase of high temperature. As for the four parameters for estimation of the reactivity, as the heating rates increase, T_{on}, v_{on} and α_1 increase, while α and especially the specific heat release keep invariant. The specific heat release that means the ability of energy release when oxidized is a characteristic parameter for a certain type of Al powders. When estimate the reactivity of Al nanopowders, it is necessary to establish a proper heating rate and make it fixed.

Acknowledgements

This work was funded by the National Natural Science Foundation of China. We would like to thank Analytical and Testing Center, Huazhong University of Science and Technology for the measurements and analysis.

References

1 Y. F. Ivanov, M. N. Osmonoliev, V. S. Sedoi, V. A. Arkhipov, S. S. Bondarchuk, A. B. Vorozhtsov, A. G. Korotkikh and V. T. Kuznetsov, Propell. Explos. Pyrot., 28 (2003) 319.
2 A. P. Ilyin, E. M. Popenko, A. A. Gromov, Y. Y. Shamina and D. V. Tikhonov, Combust. Explo. Shock Waves, 38 (2002) 665.
3 J. Zhi, W. Tian-Fang, L. Shu-Fen, Z. Feng-Qi, L. Zi-Ru, Y. Cui-Mei, L. Yang, L. Shang-Wen and Z. Gang-Zhui, J. Therm. Anal. Cal., 85 (2006) 315.
4 Y. S. Kwon, A. A. Gromov, A. P. Ilyin, E. M. Popenko and G. H. Rim, Combust. Flame, 133 (2003) 385.
5 P. E. Bocanegra, C. Chauveau and I. Gokalp, Aerosp. Sci. Technol., 11 (2007) 33.
6 D. E. G. Jones, P. Brousseau, R. C. Fouchard, A. M. Turcotte and Q. S. M. Kwok, J. Therm. Anal. Cal., 61 (2000) 805.
7 L.-J. Chen, G.-S. Li, P. Qi and L.-P. Li, J. Therm. Anal. Cal., 92 (2008) 765.
8 Z. Lin, X. Han, T. Wang and S. Li, J. Therm. Anal. Cal., 91 (2008) 709.
9 R. Sarathi, T. K. Sindhu and S. R. Chakravarthy, Mater. Charact., 58 (2007) 148.
10 D. E. G. Jones, R. Turcotte, R. C. Fouchard, Q. S. M. Kwok, A. M. Turcotte and Z. A. Qader, Propell. Explos. Pyrot., 28 (2003) 120.
11 M. A. Trunov, S. M. Umbrajkar, M. Schoenitz, J. T. Mang and E. L. Dreizin, J. Phys. Chem. B, 110 (2006) 13094.
12 Y. A. Kotov, J. Nanopart. Res., 5 (2003) 539.
13 Y. S. Kwon, Y. H. Jung, N. A. Yavorovsky, A. P. Illyn and J. S. Kim, Scripta Mater., 44 (2001) 2247.
14 A. Pivkina, D. Ivanov, Y. Frolov, S. Mudretsova, A. Nicholskaya and J. Schoonman, J. Therm. Anal. Cal., 86 (2006) 733.
15 T. M. Tillotson, A. E. Gash, R. L. Simpson, L. W. Hrubesh, J. H. Satcher and J. F. Poco, J. Non-Cryst. Solids, 285 (2001) 338.
16 L. Guo, W. Song, C. Xie, X. Zhang and M. Hu, Mater. Lett., 61 (2007) 3211.
17 S. Wang, Y. Yang, H. Yu and D. D. Dlott, Propell. Explos. Pyrot., 30 (2005) 148.
18 A. P. Ilyin, A. A. Gromov and G. V. Yablunovskii, Combust. Explo. Shock Waves, 37 (2001) 418.
19 Y. S. Kwon, J. S. Moon and A. P. Ilyin, Combust. Sci. Technol., 176 (2004) 277.

Received: June 20, 2008
Accepted: December 16, 2008

DOI: 10.1007/s10973-008-9374-7